DR. JOHN AUSTIN MOHAN (Orcid ID : 0000-0002-2758-163X)

Received Date : 19-Aug-2016

Revised Date : 25-Jan-2017

Accepted Date : 26-Jan-2017

Article type : Original Article



**Corresponding Author Email ID:** jmohan@tamu.edu

# Influence of oceanographic conditions on abundance and distribution of post-larval and juvenile carangid fishes in the northern Gulf of Mexico

**JOHN MOHAN[1], TRACEY T. SUTTON[2], APRIL B. COOK[2], KEVIN BOSWELL[3], R. J. DAVID WELLS[1,4]**

[1] *Texas A&M University at Galveston, Department of Marine Biology, 1001 Texas Clipper Rd, Galveston TX 77553*

[2] *Nova Southeastern University, Department of Marine and Environmental Sciences, 8000 North Ocean Drive, Dania Beach FL, 33004*

[3] *Florida International University, Department of Biological Sciences, 3000 NE 151st St, North Miami FL 33181*

[4] *Texas A&M University, Department of Wildlife and Fisheries Sciences, College Station, TX 77843*



**ABSTRACT**

Relationships between abundance of post-larval and juvenile carangid (jacks) fishes and physical oceanographic conditions were examined in the northern Gulf of Mexico (GoM) in 2011 with high freshwater input from the Mississippi River. Generalized additive models (GAMs) were used to explore complex relationships between carangid abundance and physical oceanographic data of sea surface temperature (SST), sea surface height anomaly (SSHA) and salinity. The five most abundant carangid species collected were: *Selene setapinnis* (34%); *Caranx crysos* (30%); *Caranx hippos* (10%); *Chloroscombrus chrysurus* (9%) and *Trachurus lathami* (8%). Post-larval carangids (median SL=10 mm) were less abundant during the spring and early summer, but more abundant during the late summer and fall, suggesting summer to fall spawning for most species. Juvenile carangid (median SL=23 mm) abundance also increased between the mid-summer and early fall. Most species showed increased abundance at lower salinities and higher temperatures, suggesting entrainment of post-larval fishes or feeding aggregations of juveniles at frontal convergence zones between the expansive river plume and dynamic mesoscale eddy water masses. However responses were species- and life-stage specific, which may indicate fine-scale habitat partitioning between species. Ordination methods also revealed higher carangid abundances at lower salinities for both post-larval and juvenile life stages, with species- and life-stage specific responses to SST and SSHA; further suggesting habitat separation between species. Results indicate strong links between physical

oceanographic features and carangid distributions in the dynamic northern GoM.

**Key words**: Carangidae, MOCNESS, Large Midwater Trawl, Generalized Additive Models, Mississippi River, Gulf of Mexico

## INTRODUCTION

Physical oceanographic features structure marine communities through bottom-up trophic interactions and passive concentration mechanisms (Lima *et al.* 2002; Meekan *et al.* 2006; Godø *et al.* 2012; Lindo-Atichati *et al.* 2012; Williams *et al.* 2015). Oceanic currents and eddies occur over diverse spatial scales and interact over various temporal scales (Hamilton 1992; Vukovich 2007). Hydrodynamic convergence and turbulent mixing supply nutrients in otherwise oligotrophic waters, fueling primary production and transferring energy to higher trophic levels (Bakun 2006). In the northern hemisphere, anticyclonic warm core eddies spin clockwise causing downwelling and are generally considered nutrient-depleted (Biggs 1992). Cyclonic cold core eddies spin counterclockwise, resulting in upwelling that introduces new nitrogen into the base of the mixed layer (Biggs 1992; Seki *et al.* 2001). Frontal zones occur at the confluence of anticyclone/cyclone eddy pairs and are often associated with increased primary and secondary production that may be advected to remote offshore locations (Toner *et al.* 2003).

The Gulf of Mexico (GoM) is a semi-enclosed intercontinental sea with unique circulation that is controlled by intrusion of the Loop Current (LC) comprising warm water from the Caribbean Sea that enters through the Yucatan Strait and exits through the Straits of Florida. As the LC extends into the eastern GoM, anticyclonic warm-core mesoscale eddies are shed and transported westward into the central and western GoM (Vukovich and Crissman 1986; Biggs 1992). Frictional interactions of warm-core eddies with the steep topography of the continental slope form cyclonic/anticyclonic eddy pairs (Hamilton 1992; Biggs and Müller-Karger 1994). The physical characteristics of mesoscale features and fronts including seas surface height anomaly (SSHA) sea surface temperature (SST), salinity and nutrient gradients influence the distribution of primary producers and subsequent secondary consumers including larval and juvenile fishes (Grimes and Finucane 1991; Rooker *et al.* 2013). Additionally, discharge from the Mississippi River, which drains two-thirds of the US continent, delivers low salinity, nutrient-rich water into the northern GoM that enhances primary and secondary productivity in

nearshore waters (Chesney *et al.* 2000; Grimes 2001). Increased nitrate and chlorophyll concentrations resulting from mesoscale circulation, are thought to support enhanced zooplankton and nekton biomass (Zimmerman & Biggs 1999) .

In the northern GoM the Mississippi River plume is a dominant feature that can extend over 400 km to offshore oceanic regions (Del Castillo *et al.* 2001). The transport of terrestrial enriched river discharge with high levels of 'new' nitrate (Dagg and Breed 2003) results in high fishery production in the northern GoM (Chesney *et al.* 2000; Grimes 2001). In 2011, record flooding of the Mississippi River with a peak discharge of 40,000 $m^3$ $s^{-1}$ in May that was twice the 60 yr mean (Walker *et al.* 2005), resulted in an expansive plume that was identifiable with satellite measurements (Falcini *et al.* 2012; Gierach *et al.* 2013). Nitrate levels recorded in the far-field plume of the Mississippi River range from 5-10 μM (Lohrenz *et al.* 1999; Dagg and Breed 2003) and are comparable to nitrate concentrations measured in cyclonic eddies in the GoM at 100 m depth ranging from 11-15 μM (Biggs and Müller-Karger 1994; Zimmerman and Biggs 1999). Thus cyclonic eddies and the river plume features may support similar levels of primary and secondary production and provide enhanced food for larval and juvenile fishes.

The Carangidae (jack) family of fishes occurs worldwide throughout tropical and temperate waters, primarily occupying the epipelagic (upper 200 m) water column. Most fishes in the family Carangidae form large schools that prey upon shrimps, squids, and other fishes while at the same time supporting the diets of large predators such as tunas, sharks, and dolphins (Torres-Rojas *et al.* 2010; Kiszka *et al.* 2014; Shimose and Wells 2015). This important family of fishes supports 5% of the annual marine finfish landings due to its value as bait, sportfish, and food in many recreational and commercial fisheries (Leak 1981; Ditty *et al.* 2004). Despite the importance of the Carangidae family, few studies have attempted to link oceanographic and environmental conditions to the distribution and abundance patterns of post-larvae and juvenile carangids in the oceanic GoM. Ditty et al. (2004) found carangid larvae were concentrated in areas of abundant zooplankton prey in the northern GoM, and suggested that dynamic frontal areas served as nurseries. Grimes & Finucane (1991) reported that carangids were the most abundant genera at river plume and shelf sampling stations in the northern GoM and hypothesized that increased feeding and growth would promote occupancy associated with river plume features. Carangids were also the most abundant species inside a river plume at the Great

Barrier Reef, Australia (Thorrold and McKinnon 1995). Given the sparse information on such an important epipelagic fish family in the GoM, we aim to examine the role of oceanic conditions on the abundance and distribution of carangid fishes in order to better predict important areas such as spawning, nursery, and feeding grounds. In addition, conditions in the northern GoM in 2011 were influenced by natural gradients of salinity due to record freshwater discharge, providing an interesting setting in which to examine carangid responses. The objectives of this study were to 1) investigate carangid abundance and distribution in relation to sea surface temperature, salinity, and sea surface height anomaly in the GoM 2) compare the responses of post-larval and juvenile carangid life stages that were collected using two gear types across spring, summer and fall seasons and 3) explore differences between the 5 most abundant carangid species collected. This information may provide important data for evaluating carangid responses to natural climate variability.

## METHODS

### *Study area and collection methods*

Collections occurred during four research cruise series totaling 160 days in the northern GoM in 2011: *Meg Skansi* A from 21 April – 29 June (N=44 stations); *Meg Skansi* B from 20 July – 28 September (N=44 stations); *Pisces* A from 23 June – 12 July (N=12 stations); and *Pisces* B from 8 September – 26 September (N=13 stations). These research expeditions were part of the larger Deepwater Horizon Natural Resource Damage Assessment (NRDA) conducted in the northern GoM (http://www.gulfspillrestoration.noaa.gov). Samples were collected aboard the R/V *Meg Skansi* using a 10-$m^2$ Multiple Opening and Closing Net and Environmental Sensing System (MOC) net (Wiebe et al. 1985; details below). The R/V *Pisces* deployed a large, dual-warp midwater trawl (LMT) net (Judkins *et al.* 2016; details below). Fish abundance was standardized by dividing the number of fishes collected by the volume of water sampled ($m^3$) for each gear type. From here on each cruise will be identified by gear type deployed (MOC or LMT) and labeled by season. For instance, *Meg Skansi* A=MOC spring/summer; *Meg Skansi* B=MOC summer/fall; *Pisces* A=LMT summer; and *Pisces* B=LMT fall.

### *R/V Meg Skansi: MOC sampling*

A 10-$m^2$ mouth area MOCNESS (3-mm mesh: MOC) net system was used due to its capability of taking discrete samples over specific depth strata. At each station, a Conductivity, Temperature, and Depth (CTD) sensor array (SBE 911 Plus; Sea-Bird Electronics, Inc.) was cast at dawn and dusk. The MOC was deployed at either 0900 h or 2100 h such that either solar noon or midnight occurred at the midpoint of the tow. The MOC sampled from 0 to 1500 m depth during descent and then sampled five depth strata discretely during retrieval: 1500-1200 m, 1200-1000 m, 1000-600 m, 600-200 m, and 200-0 m. The volume filtered by each net was calculated using an algorithm that incorporated flowmeter (TSK model) data and net angle (inclinometer), with the latter used to estimate mouth area perpendicular to tow direction. Ship speed during net deployment was approximately 1.5 knots (1 knot = ~ 0.5 m $s^{-1}$). Due to low numbers of carangid fishes collected in deep depth bins (Supporting Information: Figure 1) only collections from the surface depth bin (0-200 m) were considered for further analysis. There was no significant difference in carangid abundance between day and night samples for MOC collections for all species pooled and individual species (Supporting Information: Figure 2; Table 1), thus day and night collections were pooled for each station to correspond with daily environmental measurements from the CTD and satellites.

*R/V Pisces: LMT sampling*

The R/V *Pisces* conducted deep sampling using a large, dual-warp, high-speed pelagic trawl. The LMT is a commercial four-seam midwater trawl with minimal drag that is capable of sampling larger and more mobile species than the MOC (Judkins *et al.* 2016). The mesh size of the LMT decreases along the body of the net from 6.5 m down to 6 cm at the last panel of webbing before the codend. Net mensuration sensors and data-loggers were used to actively monitor the fishing depth of the net during the tow. Data from these sensors also provided information on wingspread and mouth opening during the tow, which was then used to calculate approximate net geometry. The LMT effective mouth area was estimated to be 165.5 $m^2$. Volume filtered was calculated using an algorithm that incorporated mouth area and the oblique distance traveled by the net. Sampling occurred over a 24-hour period using oblique tows at a speed of 5 knots from the surface to depths ranging from 700 m to a maximum of 1400 m. At each station there were two day tows and two night tows; however, there was no significant difference in carangid abundance between day and night samples for LMT collections for all

species pooled and individual species (Supporting Information: Fig. 3), thus day and night samples were pooled together for this study to correspond with daily environmental measurements from the CTD and satellites.

Once the nets were retrieved on deck, the catch was sorted into "rough" taxonomic groupings (i.e. fish families). Roughly sorted groupings were weighed on a motion-compensating scale and then preserved in 10% buffered formalin. All fishes from each station were kept and archived; nothing was discarded. Later sample processing in the laboratory involved further sorting, identification to lowest taxonomic level possible, species counts, cumulative species weights (wet weight, after blotting), and length measurements. Abundance data were standardized by effort (volume filtered, $m^3$). For the 10 $m^2$ MOC, volumes were calculated using flowmeter and net mouth angle data. The volume sampled using the LMT was two orders of magnitude larger compared to MOC cruises (Table 1); therefore abundance was multiplied by 100,000 for MOC data (expressed as individuals (ind)/$m^3$ ($x10^{-5}$)) and by 10,000,000 for LMT data (ind/$m^3$ ($x10^{-7}$)) to make values comparable for plotting purposes by displaying abundances on similar scales. Spatial and seasonal distribution and abundance of carangid species was examined by generating contoured heat maps for each cruise using the Data-Interpolating Variational Analysis (DIVA: Troupin *et al.* 2012) gridding option in Ocean Data View (ODV version 4.5.6).

*Sample processing*

All specimens collected in LMT and MOC samples were identified to the lowest possible taxonomic level, in most cases to the species level (93% of specimens). For groups that contained only a few specimens, all specimens were identified to the lowest taxonomic classification possible and measured to the nearest millimeter (mm) standard length (SL). For larger catches a subset of 25 individuals were measured. Percent occurrence of each species was calculated as the number of stations a species was present divided by the total number of stations sampled.

*Environmental data*

A CTD array was deployed at each site to record environmental variables including temperature, salinity, dissolved oxygen (DO) and fluorescence. DO and fluorescence data were

not available for every site and therefore not included in further analysis. However, the limited fluorescence data was strongly correlated to salinity (Supporting Information: Fig. 4). Measurements from the upper 1-3 m and from day and night were averaged together for daily measurements to correspond to daily satellite surface measurements. CTD salinity data were unavailable for 16% of the stations; therefore, model estimated salinity data was used to fill in data gaps (explained below) and sea surface temperature (SST) sea surface height anomaly (SSHA) was obtained exclusively from satellite data. SST measurements from the CTD were strongly correlated to remotely sensed SST values (Pearson $r^2$=0.92, p<0.0001, N=95). Remotely sensed data for each station were obtained using the Marine Geospatial Ecology Tools (MGET) in ArcGIS (v10.2) (Roberts *et al.* 2010). SSHA measurements were obtained from Aviso DUAC 2014 gridded products from merged satellites at 1/3-degree resolution. Sea surface temperature estimates were gathered from the NASA JPL PO.DAAC MODIS Aqua satellites at 1/24-degree resolution. The HYCOM & NCODA models were used to estimate surface salinity at 1/25-degree resolution. All remotely sensed data from the LMT cruises was downloaded as mean statistics using cumulative climatology bins over the dates of each cruise that encompassed less than two weeks. For MOC cruise series that spanned over three months each, remotely sensed data were downloaded as mean statistics using a monthly climatological bin type. In order to examine the spatial and temporal variability in oceanographic conditions, surface layer maps of salinity (primarily measured with CTD) SST and SSHA (satellite measurements) were created in ODV (version 4.5.6) using the weighted average gridded data display option. The weighted average gridding option was chosen as it represents discreet values of conditions measured at each station where carangid abundance was quantified and these paired measurements were used in GAM and RDA analysis.

*Statistical analysis*

Generalized Additive Models (GAMs) were used to explore relationships between carangid abundance (dependent variable) and physical oceanographic data, including salinity ( CTD measurements), SST and SSHA (satellite measurements) as continuous explanatory variables and season as a categorical factor. GAMs are versions of Generalized Linear Models that permit complex nonlinear relationships between explanatory and response variables to be

explored (Hastie and Tibshirani 1986). Abundance estimates were rounded to the nearest integer for modeling purposes. The general GAM model follows the equation:

$$E[y] = g^{-1}\left(\beta_0 + \sum_k s_k\,(x_k)\right)$$

where $E[y]$ = the expected values of the response variable, $g$ = the link function, $\beta_0$ = the intercept, $x$ represents one of $k$ explanatory variables, and $s_k$ = the smoothing function for each explanatory variable.

Due to the differences in size selectivity between MOC and LMT gear types, separate models were run for each dataset. Collinearity of explanatory variables was examined with variance inflation factors (VIF) in the *usdm* package in R version 3.0.2. The VIFs for all explanatory variables were ≤ 5 so all variables were used in the GAM models. Logarithmic links with cubic regression splines were fit with the software package *mgcv* in R. A negative binomial distribution was used due to the high abundance of zeros in the data set (Drexler and Ainsworth 2013). All models employed four degrees of freedom for each variable to prevent over fitting and reduce the risk of generating ecologically unrealistic responses (Lehmann *et al.* 2002). To explore potential effects of increased degrees of freedom, k was increased to 6, 8, and 10; however the general shape of fish-environment relationships did not change. Response plots were generated for those physical variables that were deemed to have a significant influence ($\alpha$=0.05) on abundance of carangid fishes; non-significant variables were not plotted. To examine overall model fit, percent deviance explained (DE) was calculated for each model (([null deviance – residual deviance] / null deviance) x 100).

Ordination methods were used to further examine relationships between environmental conditions and the abundance of each species. Constrained linear Redundancy Analysis (RDA) was performed in Canoco (version 5.04). The RDAs were run separately for each gear type to see if differences would be apparent between post-larval (MOC) and juvenile (LMT) life stages.

## RESULTS

*Oceanographic conditions*

During MOC–spring/summer, temperature was lower (25-26°C) in northern sites with negative (-10 to 0 cm) SSHA, but higher (>28°C) in southern central locations displaying positive (10-45 cm) SSHA (Fig. 1a, e). The greatly increased SSHA (>30 cm) and increased temperature (>29°C) suggested an extension of the LC or an anticyclonic warm core eddy that traveled in a westerly direction between MOC–spring/summer and MOC–summer/fall (Fig. 1e, f). Salinity was generally homogeneous (~36) during MOC–spring/summer except for a region of low salinity (~32) at a southern station with the highest SSHA (Fig. 1c). Decreased salinities (24-32) were evident in northern regions of MOC–summer/fall indicating a southward extension of the Mississippi River plume (Figure 1d). During MOC–summer/fall, temperatures were approximately 5°C warmer compared to MOC–spring/summer in northern and western regions, but were ~2°C cooler in eastern regions that had displayed lower SSHA (Fig. 1b, f). Similar patterns were exhibited during LMT–summer and LMT–fall cruises: lower salinities (26-32) in northern sites identified the river plume (Fig. 2c, d) and positive SSHAs (35-45 cm) from the LC extension/anticyclonic eddy shifted in a westerly direction between the LMT–summer and LMT–fall (Fig. 2e, f). For LMT–summer, warmer temperatures (30-31°C) occurred at the northern stations (Fig. 2a), while for LMT–fall warmer temperatures (~30°C) were associated with positive SSHA (~35 cm) at western stations (Fig. 2b, f). Descriptive statistics (mean ± standard deviation (SD)) and range for environmental data are presented amongst gear types and seasons (Table 1).

*Carangid abundance*

A total of 8,436 carangid fishes were collected and identified to the family level or below (Table 2). The majority of carangids were collected during the LMT sampling, comprising 26% and 60% of the total catch in the summer and fall, respectively. Fewer carangids were collected during the MOC–summer/fall (12%) and MOC–spring/summer (2%) sampling. The two most abundant species were *Selene setapinnis* (34%) and *Caranx crysos* (30%), followed by *Caranx hippos* (10%), *Chloroscombrus chrysurus* (9%), and *Trachurus lathami* (8%). The genera *Caranx* (5%) and *Selene* (1%) were next in the order of abundance and these specimens were only identified to genera-specific taxonomic levels. Eleven additional species from the

Carangidae family were also identified, but these comprised <2.8% of total abundance and thus were not included in analysis due to low sample sizes.

Carangid species displayed higher frequency of occurrence in the LMT sampling compared to the MOC sampling (Table 3). For the LMT, *S. setapinnis*, *C. crysos*, *C. hippos*, and *T. lathami* all occurred in greater than 75% of samples, while *C. chrysurus* occurred less frequently in only 26% of samples. Frequencies of occurrence of all carangid species from the MOC were generally low, ranging from 7-35%, with *C. crysos* occurring most frequently (35%) and *C. chrysurus* occurring least frequently (7%) (Table 3). Length frequency histograms revealed that smaller carangids were collected during MOC compared to LMT (Fig. 3). The median SL for MOC was 10 mm while the median SL for LMT was 23 mm. The range of carangid lengths overlapped between cruises (range MOC: 3-55 mm; range LMT: 9-149 mm), but larger fish were collected using the LMT (mean SL ± SD=27.02±15.94 mm) compared to the MOC (mean SL ± SD=12.11±6.62 mm) and this pattern was consistent for the top five most abundant species examined (Table 4).

*Carangid abundance and distribution*

Carangid abundance heat maps were created for individual species and seasonal cruises to compare abundance and distribution throughout the northern GoM (Fig. 4 and 5). For the MOC sampling *Selene setapinnis* was absent in spring/summer except for 1 individual (Fig. 4a), but in the summer/fall *S. setapinnis* displayed centralized high abundance (>60 ind/$m^3$ x$10^{-5}$) with zero abundance at western sites and increased abundance (~20 ind/$m^3$ x$10^{-5}$) at eastern sites (Fig. 4b). Similarly, *C. crysos* abundance was low in the spring/summer in south-central sites and much increased in the summer/fall with moderate abundance (20-40 ind/$m^3$ x$10^{-5}$) at single west and central sites, with higher abundance (20-80 ind/$m^3$ x$10^{-5}$) observed in the south eastern region (Fig. 4c, d). *Caranx hippos* displayed low patchy abundance (2-4 ind/$m^3$ x$10^{-5}$) for MOC in the spring/summer in the central region and high abundance in the south eastern region during the summer/fall (Fig. 4e,f). *Chloroscombrus chrysurus* was absent from spring/summer, but highly abundant (>300 ind/$m^3$ x$10^{-5}$) at one central station in the summer/fall (Fig. 4g, h). *Trachurus lathami* exhibited low abundance (2-8 ind/$m^3$ x$10^{-5}$) that shifted from the east in the spring/summer to central and western sites in the summer/fall (Fig. 4i, j).

For LMT carangid abundances were much higher in both the summer and fall compared to MOC (Fig. 5). In the summer, *S. setapinnis* was most abundant (100-150 ind/$m^3$ x$10^{-7}$) in the north-central sites, but the abundances shifted to the east sites (400 ind/$m^3$ x$10^{-7}$) during the fall but abundances remained high in the north-central (200 ind/$m^3$ x$10^{-7}$) (Fig. 5a, b). Abundances of *C. crysos* were increased (150 ind/$m^3$ x$10^{-7}$) at north-central sites in the summer and heavily concentrated (600 ind/$m^3$ x$10^{-7}$ ) at a single northern site in the fall (Fig. 5c, d). *Caranx hippos* displayed high abundance (100 ind/$m^3$ x$10^{-7}$) at northern sites in the summer that shifted to western sites in the fall (Fig. 5e, f). Abundances of *C chrysurus* were increased (100 ind/$m^3$ x$10^{-7}$) at the northern site (Fig. 5g, h) during both the summer and fall. *Trachurus lathami* exhibited moderate abundance (50 ind/$m^3$ x$10^{-7}$) at the northern site in the fall that increased and shifted to the west (200 ind/$m^3$ x$10^{-7}$) during the fall sampling (Fig. 5i, j).

*Generalized Additive Models*

Salinity was the only variable that exhibited a significant relationship to abundance for every carangid species (Table 5) however, those relationships varied between species and gear types. In general the deviance explained was high (DE>50) for each species and gear type and ranged from 45-96% (Table 5). Season of collection was also a significant factor for most species, except for *C. chysurus* and *T. lathami* LMT collections (Table 5). *Selene setapinnis* displayed increased abundance at high SSHA (>10 cm) and low salinities (<32) for MOC, however the effect of temperature was not clear (Fig. 6). For LMT, higher abundance of *S. setapinnis* was related to increased SST (>29.5°C) and decreased salinity with a dome shaped peak at salinity=29 (Fig. 6). Salinity was the only factor significantly related to *Caranx crysos* abundance and the relationship shifted between MOC and LMT, with a peak at 27 for MOC and a peak at 32 for LMT (Fig. 7). For MOC, higher *C. crysos* abundance occurred at salinities of 26-28 and for LMT there were higher abundances at salinities 30-34 (Fig. 7). SST and salinity were significantly related to *C hippos* abundance for both MOC and LMT, however the shape and direction of the relationships differed between the gears (Fig. 8). For MOC, higher *C hippos* abundance was related to decreased SST (25-28°C) and increased salinity (>35) while for LMT there were more abundant *C. hippos* at increased SST (>29.5) and decreased salinity (26-32) (Fig. 8). *Chloroscombrus chrysurus* collected with MOC exhibited increased abundance at

decreased SSHA (< 5cm), decreased salinity (26-30), and increased SST (>28°C), while *C. chysurus* collected with LMT was more abundant at low salinities (<35) (Fig. 9). For both MOC and LMT, increased *T. lathami* abundance was significantly related to increased SST (Fig. 9). For LMT, the response of *T. lathami* to salinity was variable, with increased abundance observed at moderate (27-30) and higher (>35) salinities (Fig. 9). Abundance of *T lathami* was increased at moderate SSHA (0-20 cm) for LMT (Fig. 9).

Environmental variables accounted for 27% and 20.1% of the variation in species for MOC and LMT, respectively. The RDA plots demonstrated that *S. setapinnis, C. crysos* and *C. chrysurus* all responded similarly with increased abundance at low salinities for both post-larval (Fig. 11a) and juvenile (Fig. 11b) life stages. However, the post larval stage of *S. setapinnis, C. crysos* and *C. chrysurus* were more abundant at higher temperatures, while the juvenile stages were more abundant at lower SSHA (Fig. 11). *Caranx hippos* and *T. lathami* displayed similar spatial arrangement in RDA plots for both post-larval and juvenile life stages, with higher abundances at higher SST (Fig. 11a, b).

## DISCUSSION

The northern GoM in 2011 displayed sharp gradients of SST, salinity, and SSHA, which affected the abundance and distribution of post-larval and juvenile carangids. Lower salinities that are characteristic of the Mississippi River plume, tended to result in increased abundance of most carangids, but responses to SST and SSHA were species- and life-stage specific. The seasonal sampling that encompassed the spring, summer and fall captured many gradients in oceanographic conditions that represent dominant mesoscale features in the GoM including the river plume, warm core eddies and/or the extension of the LC, and frontal regions where the eddies and the plume intersect. Additionally, the use of two gear types with different mesh size and tow speeds allowed comparison between abundance and distribution of post-larval and juvenile carangid species life stages.

Many of the studies that have examined the influence of abiotic factors on the distribution and abundance of marine fishes in the GoM have focused on larval life stages (Rooker *et al.* 2012; Kitchens and Rooker 2014; Randall *et al.* 2015). Larvae exhibit limited mobility and are

easy to collect in towed nets. Additionally, collecting larvae allows inference on spawning location and season (Shaw and Drullinger 1990; Ditty *et al.* 2004; Rooker *et al.* 2012; Kitchens and Rooker 2014). Fewer studies have focused on juvenile and sub-adult life stages of marine fishes, potentially due to high mobility of juvenile life stages and net avoidance behavior (Leak 1981). Smaller carangids were collected during MOC sampling with small mesh size (3 mm) resulting in a median fish SL of 10 mm, a size suggesting these fishes were post-larvae in a transitory phase between larvae and juvenile life stages (Aprieto 1974). Larger juvenile and sub-adult fishes with a median SL of 23 mm were collected in LMT that utilized larger mesh size (51 mm) with a 16.5X greater effective mouth area; however, both net styles did collect some carangids that were larger than 50 mm, but these subadult/adult specimens were rare. Larger carangids were collected in the LMT due to faster tow speeds of 2.6 m $s^{-1}$ compared to the MOC, which towed at speeds of 0.8 m $s^{-1}$. Leis et al. (2006) calculated *in situ* swimming speeds in larvae and early juvenile (8-18 mm SL) of a related carangid, the Giant Trevally *Caranx ignobilis,* and determined swimming speeds ranged from 2 to 20 cm $s^{-1}$ that was linearly related to SL. Therefore, applying the linear size-to-swimming speed relationship of Leis et al. (2006), a carangid juvenile of SL=50 mm could swim approximately 70 cm $s^{-1}$, or near the tow speed of the MOC net and a 100-mm juvenile would approach speeds of 140 cm $s^{-1}$. Larger carangids most likely escaped net capture by swimming faster than the net tow speed, or moving vertically or horizontally in the water column to avoid the approach of the net (Misund *et al.* 1999). Although larval and juvenile carangids prefer pelagic habitats, some adult carangids prefer benthic habitats (Clarke and Aeby 1998) and thus adults may not have been targeted by the gear types used here. Most of the carangid species examined here spawn in neritic coastal waters, where most previous surveys have focused sampling effort in shallow water < 100 m deep (Leak 1981; Shaw and Drullinger 1990; Katsuragawa and Ekau 2003; Espinosa-Fuentes and Flores-Coto 2004). In contrast, samples in this study were collected far offshore in depths ranging from 500 to 3000 m. Thus the gear types used here and areas sampled most likely captured late stage larvae to early/late juveniles that were either passively entrained in circulation patterns of the expansive river plume (Grimes and Finucane 1991; Johns *et al.* 2014) or actively engaging in ontogenetic migrations from nearshore to offshore habitats (da Costa *et al.* 2005) or aggregating in the hydrodynamic nutrient rich and productive frontal regions (Ditty *et al.* 2004; Raya and Sabates 2015).

*Abundance ranking between species*

The two most abundant species collected in this study were the *S. setapinnis* (34%) and *C. crysos* (30%), which together comprised 64% of all species collected. Few studies have reported high abundance of *S. setapinnis*, ranging from 0.2-2% of collections in the southern Atlantic off the Brazilian coast (De Souza and Junior 2008; Campos *et al.* 2010). Flores-Coto & Sanchez-Ramirez (1989) found *S. setapinnis* comprised 6.1% of collections and were most abundant in warmer months in the southern GoM, which was the highest reported abundance of *S. setapinnis* before this study. This contrasts with results of other studies in the GoM, which have typically found *C. chrysurus* to be the dominant species (Flores-Coto and Sanchez-Ramirez 1989; Ditty *et al.* 2004). Da Costa et al. (2005) examined carangid distributions in a semi-enclosed bay in southeastern Brazil and found *C. chrysurus* abundance and biomass was significantly related to decreased salinity and shallow water depths. This relationship was the result of a high number of juveniles (30-90 mm total length) collected from the inner bay which exhibited increased water temperature, low water clarity, and high organic loads that supported increased primary production and upper trophic levels (da Costa *et al.* 2005). Ditty et al (2004) sampled carangid larvae in the northern GoM and reported abundance rankings of: *C. chrysurus* 83%; *Decapterus punctatus* 9%; *C. hippos* 2.9%; *C crysos* 1.9%. *C. chrysurus* was most abundant west of the Mississippi River, while *D. punctatus* was most abundant in the eastern GoM on the Florida Shelf. *C. hippos* and *C. crysos* had similar spatial overlap, but different temporal distributions with *C. hippos* more abundant in May-June while *C. crysos* occurred more frequently in June-August (Ditty *et al.* 2004). Interestingly, we found different salinity preferences for both post-larval and juvenile *C. crysos* and *C. hippos*, suggesting spatial separation and habitat partitioning between these species. Leak (1981) sampled carangid larvae in the eastern GoM during four years and found that *D. punctatus* were over 10x more abundant than all other carangids. Shaw and Drullinger (1990) sampled carangid larvae in coastal waters of Louisiana during 1982-83 and found *C. chrysurus* was most abundant followed by *C. crysos*, *T. lathami*, and *D. punctatus* in order of abundance. In the southern GoM below 21°N, Flores-Coto & Sanchez-Ramirez (1989) examined seasonal carangid densities in 1983-84 and described ranked abundance of the same species examined here: *C. chrysurus* 54%; *D. punctatus* 16%; *T. lathami* 12%; *S. setapinnis* 6%; *C. hippos* 0.9% and *C. crysos* 0.7%. Larvae of these carangids were present year-round, except for *T. lathami*, which was only present in the winter and spring.

Several other studies have been conducted off the Brazilian coast and have found different patterns of carangid abundance (Katsuragawa and Matsuura 1992; De Souza and Junior 2008; Campos *et al.* 2010). Katsuragawa & Matsuura (1992) reported abundances of *T. lathami* 59%; *C. chrysurus* 15%; *D. punctatus* 12%, while Campos et al. (2010) reported abundances of *D. puntatus* 57%; *C. chrysurus* 17%; *C crysos* 8%, *T. lathami* 6% and *S. setapinnis* 0.2%, which was similar to the findings of De Souza & Junior (2008). The primary difference between previous work and this study was the high density of the *S. setapinnis* exhibited here, and the lack of *D. puntatus* that is typically a highly abundant carangid in the GoM and South Atlantic Ocean. *D. puntatus* spawn year-round in the eastern GoM and display more intense spawning at higher temperatures (26-32°C) and increased salinities (36-37) and perhaps were less abundant in the low salinity conditions of 2011 compared to other carangid species (Leak 1981). *D. puntatus* are also more concentrated in the eastern GoM on the Florida shelf (Leak 1981; Ditty *et al.* 2004) in an area that was not sampled in this study. Shaw and Drullinger (1990) sampled carangid larvae in coastal waters of Louisiana and found *T. lathami* was restricted to deeper depths (mean depth range 221-2768 m) and high salinities (mean salinity 36). Spawning of *T. lathami* is known to be associated with 'high amplitude event or gradients' and larvae have been collected from turbulent mixed water between the river plume and oceanic waters (Shaw and Drullinger 1990). Although *T. lathami* were found offshore in agreement with other studies, *T. lathami* presence in warmer waters has not been reported previously.

*Inferred spawning seasons and habitats*

The MOC collected post-larval carangids, which displayed consistent and narrow size ranges indicated by median SL from 8 to 17 mm TL. Most of the post-larval carangids displayed low abundance from the spring/summer samples collected in April and June, except for *T. lathami* which had comparable abundances between the seasons but different distributions. *Trachurus lathami* is the only species thought to spawn in the winter, while all the other species spawn in the summer, which would explain the higher abundance of *S. setapinnis, C. crysos, and C. chrysurus* in the summer and fall seasons (Leak 1981; Shaw and Drullinger 1990; Ditty *et al.* 2004). The post-larval abundances of three species (*S. setapinnis, C. chrysurus*, and *T. lathami*) displayed complex relationships to SST. In general there were higher abundances at increased temperatures (also evident in the RDA plot), but there was high variability in the GAM response

plots resulting in funnel shaped curves at lower temperatures. In contrast *C. hippos* post-larvae displayed a distinct peak at lower temperatures (25-28°C) and low abundance at high temperatures. *Caranx hippos* was also the only species that demonstrated increased abundance at high salinities > 35. These results suggest a separation of spawning habitat between *C. hippos* and the other carangids examined here. *Caranx hippos* was also the only species that displayed contrasting relationships between abundance and SST and salinity between post-larvae and juveniles. Additionally, the non-overlapping spatial distributions and different shapes of the salinity response plot between species may suggest a temporal or spatial succession of spawning events to reduce inter-species competition for resources (Raya and Sabates 2015). For instance, *S. setapinnis* displayed a linear salinity response plot response, while *C. crysos* and *C. chrysurus* were domed shaped and *C. hippos* was linear but negative. Species-specific responses of post-larvae abundance to SSHA were also detected. *Chloroscombrus chrysurus* abundance was increased at lower SSHA, while *S. setapinnis* was more abundant at increased SSHA, providing further evidence of habitat partitioning between species. A study of billfish spawning habitats in the northern GoM found higher densities of sailfish and swordfish larvae at low SSHA (<10 cm), but blue marlin larvae displayed increased density at high (>20 cm) and low SSHA (<-5 cm) (Rooker *et al.* 2012). Randall *et al.* (2015) reported increased bluntnose flyingfish *Prognichthys occidentalis* larvae at low SSHA (<0 cm) and high salinity (>35) and suggested the expansive river plume in 2011 may have decreased suitable spawning habitat for *P. occidentalis*, in contrast to our findings for carangids.

The commonalities and differences in species-environment relationships were also exhibited in the RDA ordination plots, where *S. setapinnis, C. crysos*, and *C. chrysurus* were correlated positively with SST and SSHA, and negatively correlated with salinity while *C. hippos* was opposite of those three species. Other studies have demonstrated that river plume features can be characterized by low salinity and increased temperature (Johns *et al.* 2014). The higher abundance of *S. setapinnis, C crysos*, and *C chrysurus* post larvae at lower salinities and warmer SST suggests association with the river plume that could either result from passive entrainment of small buoyant larvae due to hydrodynamic convergence zones (Govoni *et al.* 1989; Bakun 2006) or active seeking out of plume waters for feeding (Govoni and Chester 1990). Enhanced larval feeding may result from the photic environment of the plume, where increased suspended sediments may increase the visual contrast and overall diversity of prey

types (Govoni and Chester 1990). Dagg and Whitledge (1991) reported strong seasonality of zooplankton production in the MS River plume, with highest production occurring in the summer which concurs with our results of higher larval concentrations in the summer/fall compared to the spring/summer MOC cruises. Increased abundance of larval fishes at productive frontal zones would also attract predators, which could explain the higher occurrence of juvenile and larger carangid collected with LMT in the plume and or frontal zones. Thus perhaps some larger sized carangids (>40 mm) were inhabiting the river plume to forage on other smaller larval fish that may be entrained passively in the plume.

Juvenile carangids collected with LMT experienced a much narrower SST range (27.7-30.5°C) compared to the larval MOC SST range (24.4-31.8), which may explain the consistent linear relationship between juvenile abundance and SST for *S setapinnis*, *C. hippos* and *T lathami*. However, SST was not significantly related to *C. chrysurus* and *C. crysos* juvenile abundance. Interestingly, on the RDA plot only *C. hippos* and to a lesser extent *T. lathami* showed directional ordination with SST. Similar to the post-larval carangids, higher abundances of juvenile carangids were generally found at lower salinities and salinity was a significant variable in the GAM models for all juvenile (LMT) carangids. However, the GAM response plots was linear for *C. chrysurus*, dome-shaped for *S. setapinnis* and *C. crysos*, and S-shaped for *C. hippos* and *T. lathami*, suggesting increased abundance at both medium and high salinities. This difference was also apparent in the RDA plot, where *C. hippos* and *T. lathami* pointed in different directions than the other species, suggesting habitat partitioning between the species. The abundance heat map also identified a unique seasonal pattern for *C. hippos* and *T. lathami* (and to a lesser extent *S. setapinnis*) where the distribution shifted from the northern region in the summer to more western regions in the fall. Perhaps the westerly shifts in abundance were related to the westerly moving warm core eddy/LC extension that produced a frontal region with increased production and food availability at the intersection of the mesoscale eddy and river plume. In contrast to the post-larval carangids that may have been passively entrained in the frontal convergence zones, it is likely the larger juvenile targeted frontal zones for increased feeding (Bakun 2006). Additionally, the schooling behavior of carangid juveniles may have resulted in patchy concentrated zones (Kwei 1978) that were evident from highly localized abundance exhibited on the species heat maps.

*Conclusion*

Relationships between carangid abundance and physical oceanographic features were examined in the northern GoM in 2011, when the Mississippi River experienced record flooding. MOC and LMT gear types were used to collect fish and both *in situ* CTD and satellite measurements were used to characterize physical conditions and mesoscale features. SST, salinity, and SSHA, were related to carangid density and varied between species as a product of differences in life history strategies between post-larval and juveniles. The large expansion of the Mississippi River plume in the record-flooding year, creating frontal zones with dynamic salinity and temperature regimes that may have passively entrained post-larval carangids or aggregated foraging juveniles. Additional future studies may focus on growth measurements via otolith microstructure analyses and dietary analysis with stomach contents and tissue stable isotope analyses (Syahailatua *et al.* 2011) to examine potential resource partitioning between species over multiple years.

**ACKNOWLEDGEMENTS**

This manuscript includes both work that was conducted and samples that were collected as part of the Deepwater Horizon Natural Resource Damage Assessment being conducted cooperatively among academic partners, NOAA, other Federal and State Trustees, and BP. This research was made possible by a grant from BP/The Gulf of Mexico Research Initiative along with support by the National Oceanic and Atmospheric Administration. The findings and conclusions in this manuscript are those of the authors and do not necessarily represent the view of the National Oceanic and Atmospheric Administration or of any other natural resource trustee for the BP/Deepwater Horizon Natural Resource Damage Assessment.

## REFERENCES

Aprieto, V.L. (1974) Early development of five Carangid fishes of the Gulf of Mexico and the south Atlantic coast on the United States. *Fishery Bulletin* **72**, 415–443.

Bakun, A. (2006) Fronts and eddies as key structures in the habitat of marine fish larvae: opportunity, adaptive response and competitive advantage. *Scientia Marina* **70S2**, 105–122.

Biggs, D. (1992) Nutrients, plankton, and productivity in a awarm-core ring in the western Gulf of Mexico. *Journal of Geophysical Research* **97**, 160–163.

Biggs, D.C. and Müller-Karger, F.E. (1994) Ship and satellite observations of chlorophyll stocks in interacting cyclone-anticyclone eddy pairs in the western Gulf of Mexico. *Journal of Geophysical Research: Oceans* **99**, 7371–7384.

Campos, P.N., De Castro, M.S. and Bonecker, A.C.T. (2010) Occurrence and distribution of Carangidae larvae (Teleostei, Perciformes) from the Southwest Atlantic Ocean, Brazil (12-23oS). *Journal of Applied Ichthyology* **26**, 920–924.

Del Castillo, C.E., Coble, P.G., Conmy, R.N., Müller-Karger, F.E., Vanderbloemen, L. and Vargo, G.A. (2001) Multispectral in situ measurements of organic matter and chlorophyll fluorescence in seawater: Documenting the intrusion of the Mississippi River plume in the West Florida Shelf. *Limnology and Oceanography* **46**, 1836–1843.

Chesney, E., Baltz, D. and Thomas, R. (2000) Louisiana estuarine and coastal fisheries and habitats: perspectives from a fish's eye view. *Ecological Applications* **10**, 350–366.

Clarke, T.A. and Aeby, G.S. (1998) The use of small mid-water attraction devices for investigation of the pelagic juveniles of carangid fishes in Kaneohe Bay, Hawaii. *Bulletin of Marine Science* **62**, 947–955.

da Costa, M.R., Albieri, R.J. and Araújo, F.G. (2005) Size distribuition of the jack *Chloroscombrus chrysurus* (Linnaeus) (Actinopterygii, Carangidae) in a tropical bay at southeastern Brazil. *Revista Brasileira de Zoologia* **22**, 580–586.

Dagg, M.J. and Breed, G.A. (2003) Biological effects of Mississippi River nitrogen on the northern Gulf of Mexico - A review and synthesis. *Journal of Marine Systems* **43**, 133–152.

Dagg, M.J. and Whitledge, T.E. (1991) Concentrations of copepod nauplii associated with the nutrient-rich plume of the Mississippi River. *Continental Shelf Research* **11**, 1409–1423.

Ditty, J.G., Shaw, R.F. and Cope, J.S. (2004) Distribution of carangid larvae (Teleostei: Carangidae) and concentrations of zooplankton in the northern Gulf of Mexico, with illustrations of early *Hemicaranx amblyrhynchus* and Caranx spp. larvae. *Marine Biology* **145**, 1001–1014.

Drexler, M. and Ainsworth, C.H. (2013) Generalized additive models used to predict species abundance in the Gulf of Mexico: an ecosystem modeling tool. *PLoS ONE* **8**, e64458.

Espinosa-Fuentes, M.L. and Flores-Coto, C. (2004) Cross-shelf and vertical structure of ichthyoplankton assemblages in continental shelf waters of the Southern Gulf of Mexico. *Estuarine, Coastal and Shelf Science* **59**, 333–352.

Falcini, F., Khan, N.S., Macelloni, L., et al. (2012) Linking the historic 2011 Mississippi River flood to coastal wetland sedimentation. *Nature Geoscience* **5**, 803–807.

Flores-Coto, C. and Sanchez-Ramirez, M. (1989) Larval distribution and abundance of Carangidae (Pisces), from the southern Gulf of Mexico. 1983-1984. *Gulf Research Reports* **8**, 117–128.

603 Gierach, M.M., Vazquez-Cuervo, J., Lee, T. and Tsontos, V.M. (2013) Aquarius and SMOS
604 detect effects of an extreme Mississippi River flooding event in the Gulf of Mexico.
605 *Geophysical Research Letters* **40**, 5188–5193.

606 Godø, O.R., Samuelsen, A., Macaulay, G.J., et al. (2012) Mesoscale eddies are oases for higher
607 trophic marine life. *PLoS ONE* **7**, e30161.

608 Govoni, J. and Chester, A. (1990) Diet composition of larval *Leistomus xanthurus* in and about
609 the Mississippi River plume. *Journal of Plankton Research* **12**, 819–830.

610 Govoni, J.J., Hoss, D.E. and Colby, D.R. (1989) The spatial distribution of larval fishes about the
611 Mississippi River plume. *Limnology and Oceanography* **34**, 178–187.

612 Grimes, C. (2001) Fishery production and the Mississippi River discharge. *Fisheries* **26**, 17–26.

613 Grimes, C. and Finucane, J. (1991) Spatial distribution and abundance of larval and juvenile fish,
614 chlorophyll and macrozooplankton around the Mississippi River discharge plume, and the
615 role of the plume in fish recruitment. *Marine Ecology Progress Series* **75**, 109–119.

616 Hamilton, P. (1992) Lower continental slope cyclonic eddies in the central Gulf of Mexico.
617 *Journal of Geophysical Research* **97**, 2185–220.

618 Hastie, T.J. and Tibshirani, R. (1986) Generalized additive models. *Statistical Science* **1**, 297–
619 318.

620 Johns, E.M., Muhling, B.A., Perez, R.C., et al. (2014) Amazon River water in the northeastern
621 Caribbean Sea and its effect on larval reef fish assemblages during April 2009. *Fisheries*
622 *Oceanography* **23**, 472–494.

623 Judkins, H., Vecchione, M., Cook, A. and Sutton, T. (2016) Diversity of midwater cephalopods
624 in the northern Gulf of Mexico: comparison of two collecting methods. *Marine Biodiversity*.

625 Katsuragawa, M. and Ekau, W. (2003) Distribution, growth and mortality of young rough scad,
626 *Trachurus lathami*, in the south-eastern Brazilian Bight. *Journal of Applied Ichthyology* **19**,
627 21–28.

Katsuragawa, M. and Matsuura, Y. (1992) Distribution and abundance of carangid larvae in the southeastern Brazilian Bight during 1975-1981. *Bolm Inst. oceanogr., S Paulo* **40**, 55–78.

Kiszka, J.J., Méndez-Fernandez, P., Heithaus, M.R. and Ridoux, V. (2014) The foraging ecology of coastal bottlenose dolphins based on stable isotope mixing models and behavioural sampling. *Marine Biology* **161**, 953–961

Kitchens, L.L. and Rooker, J.R. (2014) Habitat associations of dolphinfish larvae in the Gulf of Mexico. *Fisheries Oceanography*, 1–12.

Kwei, E.A. (1978) Food and spawning activity of *Caranx hippos* off the coast of Ghana. *Journal of Natural History* **12**, 195–215.

Leak, J.C. (1981) Distribution and abundance of Carangid fish larvae in the Eastern Gulf of Mexico, 1971-1974. *Biological Oceanography* **1**, 1–28.

Lehmann, A., Overton, J.M.C. and Leathwick, J.R. (2002) GRASP: generalized regression analysis and spatial prediction. *Ecological Modelling* **157**, 189–207.

Leis, J.M., Hay, A.C., Clark, D.L., Chen, I.S. and Shao, K.T. (2006) Behavioral ontogeny in larvae and early juveniles of the giant trevally (*Caranx ignobilis*) (Pisces: Carangidae). *Fishery Bulletin* **104**, 401–414.

Lima, I.D., Olson, D.B. and Doney, S.C. (2002) Biological response to frontal dynamics and mesoscale variability in oligotrophic environments: Biological production and community structure. *Journal of Geophysical Research* **107**, 1–21.

Lindo-Atichati, D., Bringas, F., Goni, G., Muhling, B., Muller-Karger, F.E. and Habtes, S. (2012) Varying mesoscale structures influence larval fish distribution in the northern Gulf of Mexico. *Marine Ecology Progress Series* **463**, 245–257.

Lohrenz, S.E., Fahnenstiel, G.L., Redalje, D.G., Lang, G.A., Dagg, M.J., Whitledge, T.E. and Dortch, Q. (1999) Nutrients, irradiance, and mixing as factors regulation primary production in coastal waters impacted by the Mississippi River plume. *Continental Shelf Research* **19**, 1113–1141.

Meekan, M.G., Carleton, J.H., Steinberg, C.R., et al. (2006) Turbulent mixing and mesoscale distributions of late-stage fish larvae on the NW Shelf of Western Australia. *Fisheries Oceanography* **15**, 44–59.

Misund, O., Luyeye, N., Coetzee, J. and Boyer, D. (1999) Trawl sampling of small pelagic fish off Angola: effects of avoidance, towing speed, tow duration, and time of day. *ICES Journal of Marine Science* **56**, 275–283.

Randall, L.L., Smith, B.L., Cowan, J.H. and Rooker, J.R. (2015) Habitat characteristics of bluntnose flyingfish *Prognichthys occidentalis* (Actinopterygii, Exocoetidae), across mesoscale features in the Gulf of Mexico. *Hydrobiologia* **749**, 97–111.

Raya, V. and Sabates, A. (2015) Diversity and distribution of early life stages of carangid fishes in the northwestern Mediterranean: responses to environmental drivers. *Fisheries Oceanography* **24**, 118–134.

Roberts, J.J., Best, B.D., Dunn, D.C., Treml, E.A. and Halpin, P.N. (2010) Marine Geospatial Ecology Tools: An integrated framework for ecological geoprocessing with ArcGIS, Python, R, MATLAB, and C++. *Environmental Modelling and Software* **25**, 1197–1207.

Rooker, J.R., Kitchens, L.L., Dance, M.A., Wells, R.J.D., Falterman, B. and Cornic, M. (2013) Spatial, temporal, and habitat-related variation in abundance of pelagic fishes in the Gulf of Mexico: potential implications of the Deepwater Horizon Oil Spill. *PLoS ONE* **8**, e76080.

Rooker, J.R., Simms, J.R., David Wells, R.J., Holt, S.A., Holt, G.J., Graves, J.E. and Furey, N.B. (2012) Distribution and habitat associations of billfish and swordfish larvae across mesoscale features in the Gulf of Mexico. *PLoS ONE* **7**, e34180.

Seki, M.P., Polovina, J.J., Brainard, R.E., Bidigare, R.R., Leonard, C.L. and Foley, D.G. (2001) Biological enhancement at cyclonic eddies tracked with GOES thermal imagery in Hawaiian waters. *Geophysical Research Letters* **28**, 1583–1586.

Shaw, R.F. and Drullinger, D.L. (1990) Early-Life-History profiles, seasonal abundance, and distribution of four Species of Carangid larvae from the Northern Gulf of Mexico, 1982 and 1983.

681 Shimose, T. and Wells, R. (2015) Feeding Ecology of Bluefin Tunas. In: *Biology and Ecology of*
682 *Bluefin Tunas*. (eds T. Kitagawa and S. Kumura). CRC Press, Taylor and Francis Group, pp
683 78–97.

684 De Souza, C.S. and Junior, P.M. (2008) Distribution and abundance of Carangidae (Teleostei,
685 Perciformes) associated with oceanographic factors along the Northeast Brazilian Exclusive
686 Economic Zone. *Brazilian Archives of Biology and Technology* **51**, 1267–1278.

687 Syahailatua, A., Taylor, M.D. and Suthers, I.M. (2011) Growth variability and stable isotope
688 composition of two larval carangid fishes in the East Australian Current: The role of
689 upwelling in the separation zone. *Deep-Sea Research Part II* **58**, 691–698.

690 Thorrold, S. and McKinnon, A. (1995) Response of larval fish assemblages to a riverine plume
691 in coastal waters of the central great barrier reef lagoon. *Limnology and Oceanography* **40**,
692 177–181.

693 Torres-Rojas, Y.E., Hernández-Herrera, A., Galván-Magaña, F. and Alatorre-Ramírez, V.G.
694 (2010) Stomach content analysis of juvenile, scalloped hammerhead shark *Sphyrna lewini*
695 captured off the coast of Mazatlan, Mexico. *Aquatic Ecology* **44**, 301–308.

696 Toner, M., Kirwan, A., Poje, A., Kantha, L., Muller-Karger, F. and Jones, C. (2003) Chlorophyll
697 dispersal by eddy-eddy interactions in the Gulf of Mexico. *Journal of Geophysical*
698 *Research* **108**, 1–12.

699 Troupin, C., Barth, A., Sirjacobs, D., et al. (2012) Generation of analysis and consistent error
700 fields using the Data Interpolating Variational Analysis (DIVA). *Ocean Modelling* **52**–**53**,
701 90–101.

702 Vukovich, F.M. (2007) Climatology of ocean features in the Gulf of Mexico using satellite
703 remote sensing data. *Journal of Physical Oceanography* **37**, 689–707.

704 Vukovich, F.M. and Crissman, B.W. (1986) Aspects of warm rings in the Gulf of Mexico.
705 *Journal of Geophysical Research* **91**, 2645–2660.

706 Walker, N.D., Wiseman, W.J., Rouse, L.J. and Babin, A. (2005) Effects of river discharge, wind

stress, and slope eddies on circulation and the satellite-observed structure of the Mississippi River Plume. *Journal of Coastal Research* **216**, 1228–1244.

Wiebe, P., Morton, A., Bradley, A., et al. (1985) New developments in the MOCNESS, an apparatus for sampling zooplankton and micronekton. *Marine Biology* **87**, 313–323.

Williams, A.K., Mcinnes, A.S., Rooker, J.R. and Quigg, A. (2015) Changes in microbial plankton assemblages induced by mesoscale oceanographic features in the northern Gulf of Mexico. *PLoS ONE*, 1–21.

Zimmerman, R.A. and Biggs, D.C. (1999) Patterns of distribution of sound-scattering zooplankton in warm- and cold-core eddies in the Gulf of Mexico, from a narrowband acoustic Doppler current profiler survey. *Journal of Geophysical Research* **104**, 5251–5262.

**Table 1.** Summary statistics of mean (± SD) and range of physical factors measured with CTD (salinity), and satellite (SST and SSHA) at each station during each research cruise using the MOCNESS and LMT during the spring, summer and fall of 2011.

| Physical factor | statistic | Research cruise | | | |
|---|---|---|---|---|---|
| | | MOCNESS spring/ summer | LMT summer | MOCNESS summer/ fall | LMT fall |
| Temperature (℃) | mean | 26.9 ± 1.7 | 29.5 ± 0.43 | 30.5 ± 0.95 | 28.9 ± 2.2 |
| | range | 24.4 to 29.7 | 29.1 to 30.5 | 28.6 to 31.8 | 27.7 to 29.5 |
| Salinity | mean | 36 ± 1 | 34.5 ± 3.3 | 33.6 ± 2.7 | 35.3 ± 2.2 |
| | range | 31.5 to 36.7 | 24.6 to 36.4 | 23 to 36.3 | 28.8 to 36.7 |
| SSHA (cm) | mean | 6.6 ± 12.8 | 24.4 ± 15.6 | 16.4 ± 11 | 14.6 ± 10.8 |
| | range | -11.5 to 42.3 | 3.7 to 46.7 | -0.36 to 48.7 | 3.7 to 38.5 |

**Table 2.** Total numbers of carangid fishes (by genera and species) collected in the northern GoM using MOCNESS and LMT gear types during the spring, summer and fall seasons. Total sum and average volume of water column sampled during each cruise also presented. Carangids listed highest to lowest based on total abundance.

| Species | Research cruise | | | | Grand Total |
|---|---|---|---|---|---|
| | MOCNESS spring/ summer | LMT summer | MOCNESS summer/ fall | LMT fall | |
| *Selene setapinnis* | 1 | 425 | 258 | 2143 | 2827 |
| *Caranx crysos* | 2 | 663 | 252 | 1611 | 2528 |
| *Caranx hippos* | 11 | 409 | 20 | 411 | 851 |
| *Chloroscombrus chrysurus* | | 130 | 357 | 254 | 741 |
| *Trachurus lathami* | 5 | 118 | 6 | 518 | 647 |
| *Caranx* sp. | 96 | 314 | 42 | 8 | 460 |
| *Selene* sp. | 30 | | 78 | 1 | 109 |
| *Caranx bartholomaei* | | 31 | 3 | 30 | 64 |
| *Selar crumenophthalmus* | 1 | 43 | 4 | 2 | 50 |
| *Decapterus* sp. | 3 | 27 | | 10 | 40 |
| *Selene brownii* | | | | 36 | 36 |
| *Decapterus macarellus* | 15 | 12 | | 1 | 28 |
| *Decapterus tabl* | 6 | 12 | | 2 | 20 |
| *Caranx ruber* | | 12 | | | 12 |
| *Decapterus punctatus* | | | 9 | | 9 |

| | | | | | |
|---|---|---|---|---|---|
| *Alectis ciliaris* | | | 4 | 1 | 5 |
| *Selene vomer* | | 3 | 1 | | 4 |
| *Uraspis secunda* | | 3 | | 1 | 4 |
| *Pseudocaranx dentex* | | | 1 | | 1 |
| **Grand Total** | **170** | **2202** | **1035** | **5029** | **8436** |
| Total sum of volume sampled | 1,378,606 | 110,127,577 | 1,927,156 | 113,497,582 | |
| Mean Volume sampled | 49,236 | 9,177,298 | 52,085 | 8,730,583 | |

* Specimens only identified to Genus level due to morphological damage

733

734

735 **Table 3.** Frequency of occurrence for each of the most common carangid species collected using
736 MOCNESS and LMT gear.

| Cruise | Carangid frequency of occurrence (%) | | | | | |
|---|---|---|---|---|---|---|
| | *S. setapinnis* | *C. crysos* | *C. hippos* | *C. chryurus* | *T. lathami* | Species pooled |
| MOCNESS | 26 | 35 | 10 | 7 | 8 | 70 |
| LMT | 76 | 88 | 76 | 28 | 76 | 100 |

737

738

739 **Table 4.** Summary of total length (TL) measurements (mm) for each carangid species collected
740 using MOCNESS of LMT gear. N=sample size of measured fish; SD=standard deviation. Size-
741 frequency distribution presented in Figure 3.

| Cruise | species | N | minimum | maximum | median | mean ± SD |
|---|---|---|---|---|---|---|
| MOC | *S. setapinnis* | 248 | 3 | 43 | 9 | 9.54±3.98 |
| | *C. crysos* | 231 | 4 | 55 | 11 | 12.91±6.55 |
| | *C. hippos* | 31 | 4 | 20 | 8 | 8.77±2.98 |
| | *C. chrysurus* | 73 | 6 | 54 | 17 | 19.27±8.97 |
| | *T. lathami* | 13 | 6 | 24 | 16 | 14.54±4.86 |
| | combined | 596 | 3 | 55 | 10 | 12.11±6.62 |

| | | | | | | |
|---|---|---|---|---|---|---|
| LMT | *S. setapinnis* | 1104 | 9 | 66 | 20 | 22.15±8.56 |
| | *C. crysos* | 949 | 10 | 142 | 26 | 32.27±21.6 |
| | *C. hippos* | 605 | 11 | 92 | 21 | 21.31±6.79 |
| | *C. chrysurus* | 142 | 13 | 67 | 27 | 29.21±10.26 |
| | *T. lathami* | 298 | 17 | 149 | 35 | 38.88±18.89 |
| | combined | 3098 | 9 | 149 | 23 | 27.02±15.94 |

**Table 5.** Generalized Additive Model (GAM) results demonstrating the influence of season and physical factors on the five most abundant carangid species collected during MOCNESS and LMT sampling. Significant variables ($p<0.05$) in bold and percent deviance explained (DE) for each model is presented.

| Cruise | Species | Factor | | | | DE (%) |
|---|---|---|---|---|---|---|
| | | Season | SSHA | SST | Salinity | |
| MOCNESS | *S. setapinnis* | **<0.0001** | **0.0005** | **<0.0001** | **<0.0001** | 69 |
| | *C. crysos* | **<0.0001** | 0.2191 | 0.0516 | **0.0092** | 53 |
| | *C. hippos* | **0.0007** | 0.0471 | **0.0092** | **0.0086** | 53 |
| | *C. chrysurus* | ***I*** | **0.0001** | **<0.0001** | **<0.0001** | 96 |
| | *T. lathami* | **0.0007** | 0.1926 | **0.0064** | 0.5338 | 51 |
| LMT | *S. setapinnis* | **<0.0001** | 0.1840 | **0.0000** | **<0.0001** | 63 |
| | *C. crysos* | **0.0001** | 0.0926 | 0.0745 | **0.0099** | 45 |
| | *C. hippos* | **0.0343** | 0.6130 | **0.0000** | **<0.0001** | 51 |
| | *C. chrysurus* | 0.2950 | 0.2322 | 0.1142 | **0.0322** | 95 |
| | *T. lathami* | 0.0784 | **0.0002** | **0.0002** | **<0.0001** | 71 |

753

754

755

756

757 **Figure captions**

758 **Figure 1.** Physical oceanographic conditions of temperature (SST) (a, b), salinity (c, d), and sea
759 surface height anomaly (SSHA) (e, f) present during MOCNESS sampling in the spring/early
760 summer and late summer/fall of 2011. Colors represent weighted average gridding in ODV.

761 **Figure 2.** Physical oceanographic conditions of temperature (SST) (a, b), salinity (c, d), and sea
762 surface height anomaly (SSHA) (e, f) present during LMT sampling in the summer and fall of
763 2011. Colors represent weighted average gridding in ODV.

764 **Figure 3.** Size frequency distribution for each carangid species collected using MOCNESS (red)
765 and LMT (blue) gear types.

766 **Figure 4.** Density distribution heat maps (ind/$m^3$ $10^{-5}$) for *Selene setapinnis* (a, b), *Caranx crysos*
767 (c, d) and *Caranx hippos* (e, f) *Chloroscombrus chrysurus* (g, h) and *Trachurus lathami* (i, j)
768 collected during the MOCNESS sampling in the spring/summer and summer/fall. Colors
769 represent DIVA gridding in ODV; note difference in sample size (*N*) and scale bar for each plot.

770 **Figure 5.** Density distribution heat maps (ind/$m^3$ $10^{-7}$) for *Selene setapinnis* (a, b), *Caranx crysos*
771 (c, d) and *Caranx hippos* (e, f) *Chloroscombrus chrysurus* (g, h) and *Trachurus lathami* (i, j)
772 collected during the LMT sampling in the summer and fall. Colors represent DIVA gridding in
773 ODV; note difference in sample size (*N*) and scale bar for each plot.

774 **Figure 6.** Response plots for *Selene setapinnis* abundance in relation to sea surface temperature
775 (SST), sea surface height anomaly (SSHA) and salinity determined from GAM models for fish
776 collected using MOCNESS (MOC) and large midwater trawls (LMT). Non-significant variables
777 not plotted.

778 **Figure 7.** Response plots for *Caranx crysos* abundance in relation sea surface temperature

(SST), sea surface height anolomy (SSHA) and salinity determined from GAM models for fish collected using MOCNESS (MOC) and large midwater trawls (LMT). Non-significant variables not plotted.

**Figure 8.** Response plots for *Caranx hippos* abundance in relation sea surface temperature (SST), sea surface height anolomy (SSHA) and salinity determined from GAM models for fish collected using MOCNESS (MOC) and large midwater trawls (LMT). Non-significant variables not plotted.

**Figure 9.** Response plots for *Chloroscombrus chrysos* abundance in relation sea surface temperature (SST), sea surface height anolomy (SSHA) and salinity determined from GAM models for fish collected using MOCNESS (MOC) and large midwater trawls (LMT). Non-significant variables not plotted.

**Figure 10**. Response plots for *Trachurus lathami* abundance in relation sea surface temperature (SST), sea surface height anolomy (SSHA) and salinity determined from GAM models for fish collected using large midwater trawls (LMT). Non-significant variables not plotted.

**Figure 11**. Redundancy analysis (RDA) plots exploring relationships between environmental factors (red arrows) and species abundance (weighted average = triangles) for MOCNESS (a) and LMT (b) collected samples.

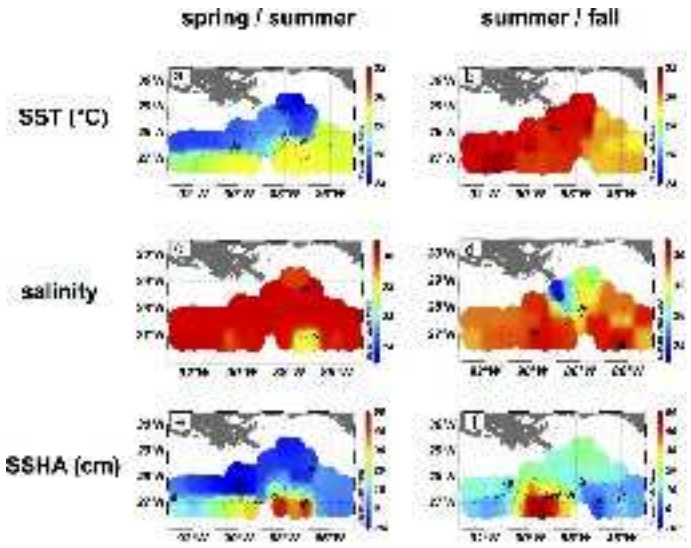


fog_12214_f1.tiff

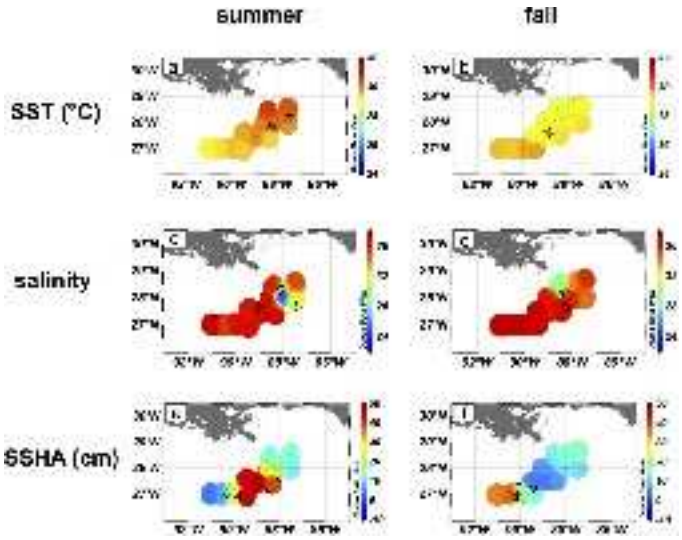


fog_12214_f2.tiff

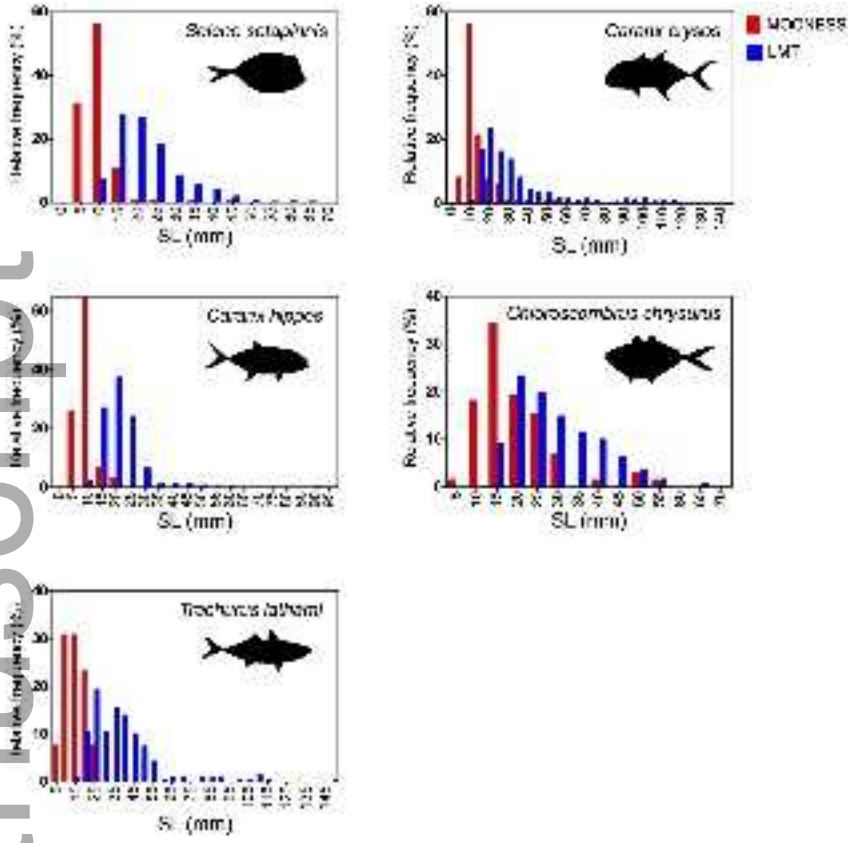


fog_12214_f3.tiff

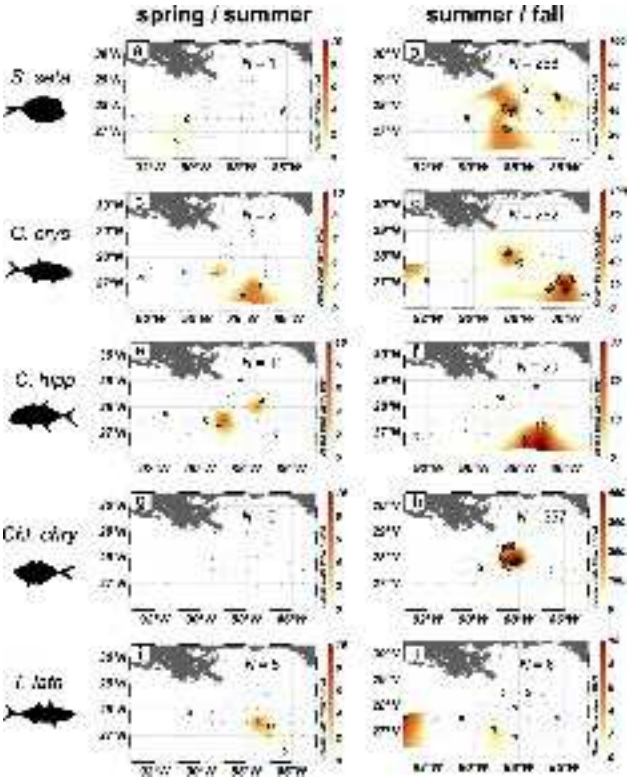


fog_12214_f4.tiff

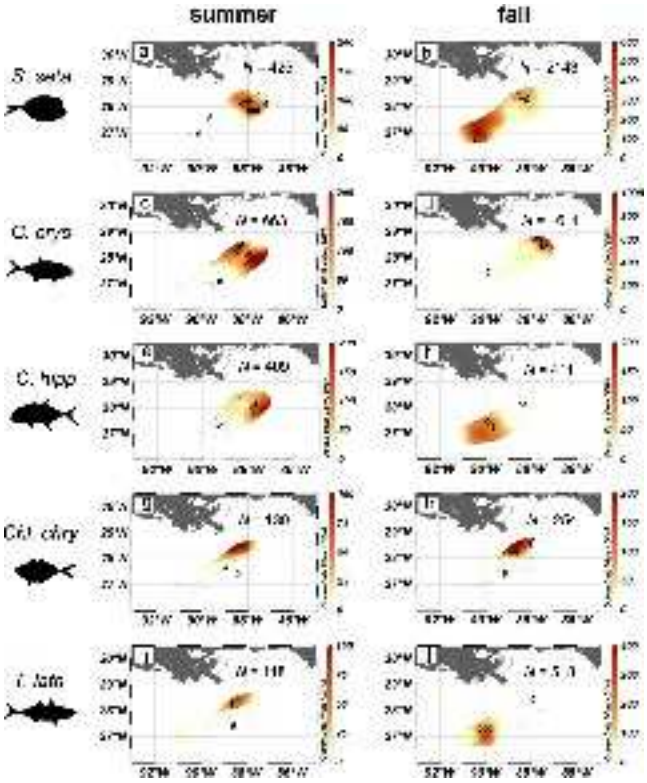


fog_12214_f5.tiff

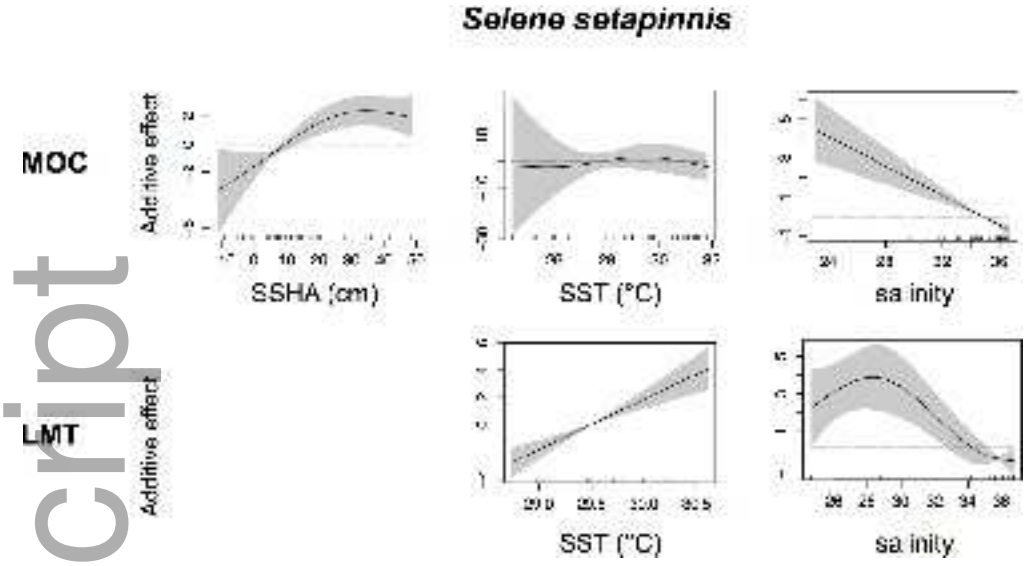


fog_12214_f6.tiff


fog_12214_f7.tiff

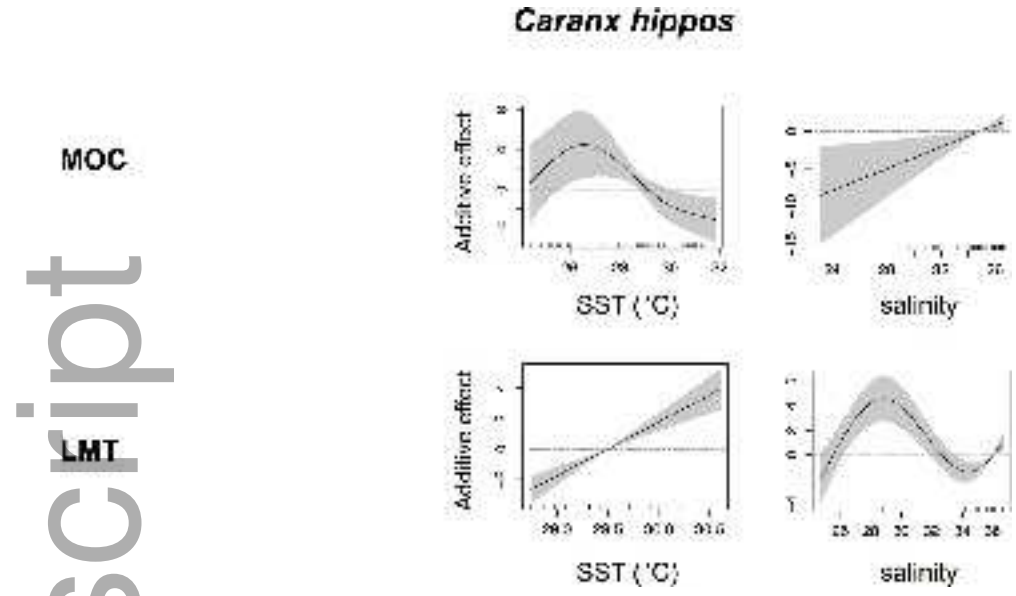


fog_12214_f8.tiff

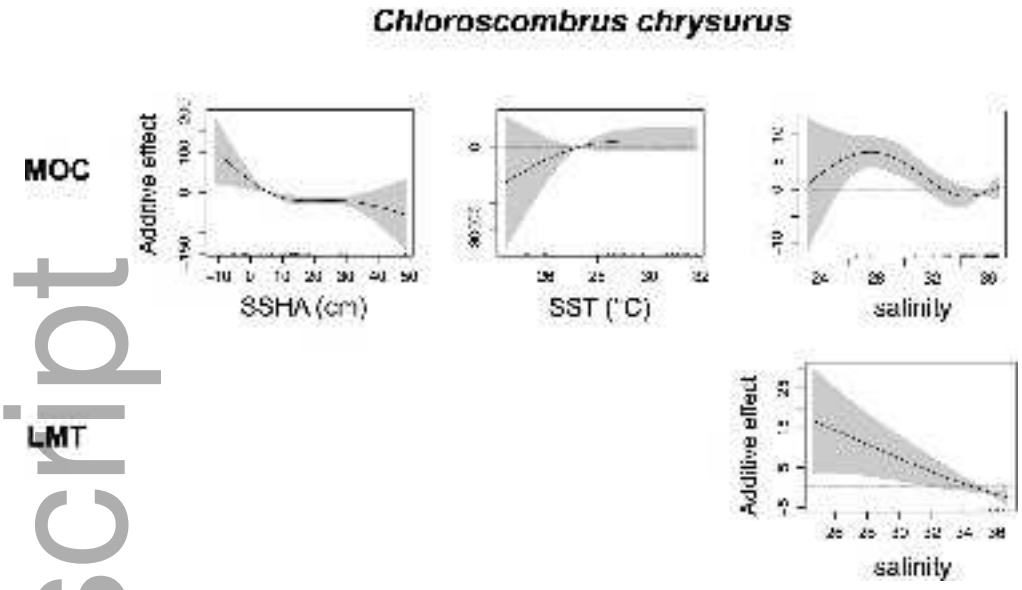


fog_12214_f9.tiff

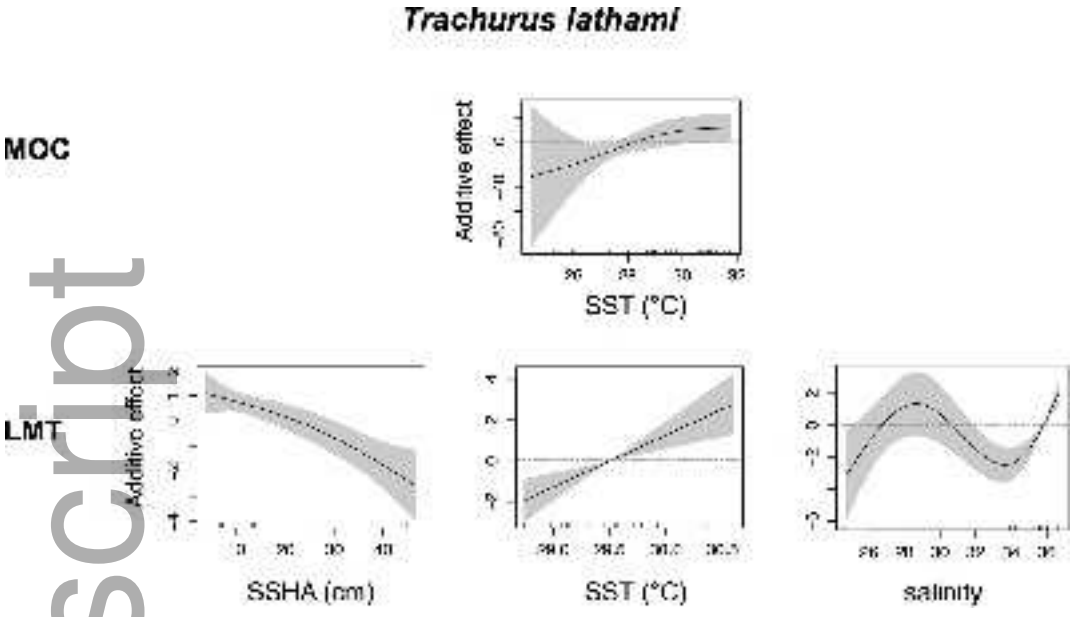


fog_12214_f10.tiff

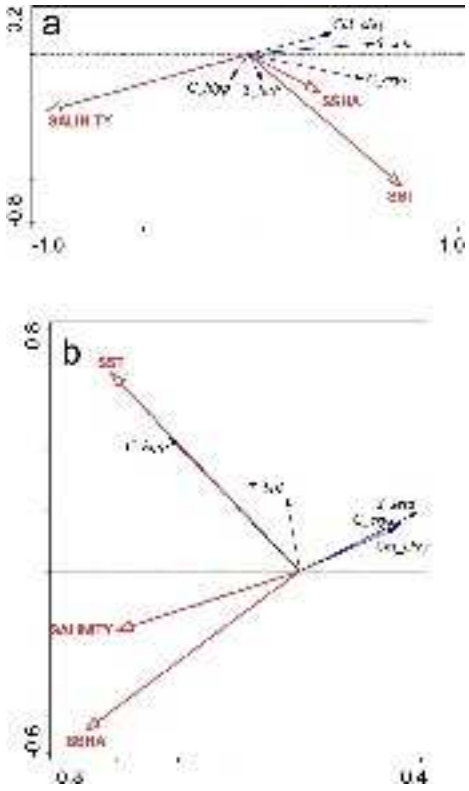


fog_12214_f11.tiff